

Removal of Hg (I) and Hg (II) Ions from Aqueous Solutions, Using TiO₂ Nanoparticles

Afshar, E.¹, Mohammadi-Manesh, H.¹ and Dashti Khavidaki, H.^{2*}

1. Department of Chemistry, Yazd University, Yazd, Iran

2. Department of Chemistry, Ayatollah Aozma Boroujerdi University, Boroujerd, Iran

Received: 16 Feb. 2017

Accepted: 8 Apr. 2017

ABSTRACT: For the first time, the present study removes ions of mercury, in the form of Hg (I) and Hg (II) ions, from aqueous solutions by adsorbing them onto titanium dioxide nanoparticles. The effects of various parameters, such as solution's initial pH, temperature, sorbent dosage, initial mercury concentration, and contact time have been examined on the adsorption process. The experimental results have been compared with Langmuir, Freundlich, and Temkin adsorption isotherms. The maximum adsorption, obtained for Hg (I) and Hg (II) ions, have been 97.5% and 98.6%, respectively. Also, it has been shown that the Langmuir isotherm has better fitting with the equilibrium data than the Freundlich and Temkin isotherms. Thermodynamic parameters of the adsorption, such as ΔH^0 and ΔS^0 have been calculated, the negative values of which show that the mercury ions adsorption is an exothermic process and that randomness is decreased, respectively. The study of adsorption kinetics shows that the adsorption of Hg (I) and (II) ions with TiO₂ nanoparticles is pseudo-second order.

Keywords: adsorption, adsorption isotherms, heavy metals, maximum adsorption capacity, nano-adsorbents.

INTRODUCTION

As a result of industrial development, increasing urban sewage and industrial pollution with toxic compounds has become a main concern. Among the toxic substances, released by industrial activities, heavy metals threaten aquatic life the most, owing to their non-degradable nature, severe toxicity, and carcinogenicity and aggregation capabilities (Ok et al., 2007). Mercury is one of the heavy metals and very toxic. Mercury compounds are toxic and impossible contaminations in environment (Farooq et al., 2010). Mercury is classified into three main groups: elemental, inorganic, and

organic mercury (Bernhoft, 2012). Elemental mercury is used in thermometer, metallurgy, mining, gold extraction, and dentistry (Nriagu et al., 1992; Pestana & Formoso, 2003). It is poorly absorbed, presenting little health risk, yet in the vapor form, metallic mercury is readily absorbed through the lungs and can cause body damage (Houston, 2007). Inorganic mercury compounds, such as mercury salts, result from the combination of mercury with chlorine, sulfur, or oxygen. Mercuric chloride (HgCl₂), used as a preservative for photographic development, is highly toxic and corrosive; mercury sulfide (HgS) is often used as a pigment in paints due to its red color; and mercury fulminate (Hg(CNO)₂) is used as an explosive

* Corresponding author Email: dashti@abru.ac.ir

detonator (Azevedo et al., 2012; Geier & Geier, 2003). Like elemental mercury, the inorganic one in the blood stream binds to erythrocytes and amino acids, disrupting their activities, causing glutathione or metallothionein, or it is transported suspended in plasma (Ballatori & Clarkson, 1985; Grandjean et al., 1997). Organic mercury compounds result from a covalent bond between mercury and carbon atoms of an organic functional group such as a methyl, ethyl, or phenyl group. Methyl mercury is often formed by methylation of inorganic mercuric ions by soil and water microorganisms (Zalups, 2000; Clarkson & Magos, 2006; Rooney, 2007). The highest amount of a mercury compound to exist in human body is in the form of methyl mercury, which usually enters human body by eating fish (Namasivayam & Kadirvelu, 1999; Bae et al., 2001).

High exposure to mercury induces changes in the central nervous system, potentially resulting in irritability, fatigue, behavioral changes, tremors, headaches, hearing and cognitive loss, dysarthria, incoordination, and hallucinations (Azevedo et al., 2012). Also, the mercury compounds harm the liver and kidneys, causing some disorder in enzymic activity, resulting in illness and death (Wagner-Dobler et al., 2000; Boening, 2000).

Several methods have been proposed to remove mercury from water (Saglam et al., 1999; Hunsom et al., 2005; El-Samrani et al., 2008; Yun et al., 1993; Dabrowski, 2001; Ozaki et al., 2002; Yaghmaeian et al., 2015; Rahmanzadeh et al., 2016; Wang et al., 2016). These methods must be considered in terms of their feasibility and cost, in addition to the acceptable impact of the removing the mentioned material. Adsorption is a useful method to remove mercury ions from aqueous solutions (Fu & Wang, 2011). In this study, mercury ions, in the form of Hg (I) and Hg (II) ions, in aqueous solutions are adsorbed by titanium dioxide nanoparticles, for the first time.

MATERIALS AND METHODS

Mercury (I) nitrate ($\text{Hg}_2(\text{NO}_3)_2 \cdot 2\text{H}_2\text{O}$) and Mercury (II) nitrate ($\text{Hg}(\text{NO}_3)_2 \cdot \text{H}_2\text{O}$) were purchased from Merck, Germany. Titanium dioxide nanoparticles (Rutile/Anatase: 85/15, Purity: >99%, Average Particle Size (APS): 20 nm, Specific Surface Area (SSA): >30 m^2/g) were prepared from Degussa. In the experiment, 50 ml of Hg (I) and Hg (II) ions solution with a certain concentration, determined via dilution of the stock solution, was poured into a 100 ml flask. In order to adjust the solution's pH, we used optimum amount of NaOH or HCl 1, i.e. 0.5 or 0.01 M solution. Then, a given mass of TiO_2 nanoparticles was added to each flask and the resultant suspension was shaken in a thermostatic orbit incubator shaker for 45 min. Once completed, a sample of the suspension was removed from the flask and filtered with a filter paper to separate adsorbent particles. The filtrate was analyzed for residual Hg(I) and Hg(II) ions. The adsorption percentage (% adsorption) was determined as:

$$\% \text{Adsorption} = \frac{C_i - C_f}{C_i} \times 100 \quad (1)$$

where C_i (mg/L) is the initial concentration of Hg(I) and Hg(II) ions and C_f (mg/L), the final concentration of Hg(I) and Hg(II) ions in the solution. The quantity of mercury ions adsorbed per unit mass of adsorbent (q_e) was obtained, using Equation (2) (Fakhri, 2015).

$$q_e = \frac{v}{m} (C_i - C_e) \quad (2)$$

where C_i is the initial concentration of Hg(I) and Hg(II) ions and C_e (mg/L), the equilibrium concentration of Hg(I) and Hg(II) ions in the solution. The solution's volume is represented with v (L) while m (g) stands for the adsorbent's mass.

RESULTS AND DISCUSSION

One of the most important parameters in adsorption process is the initial pH of the solution. For mercury ions (I) and (II), this value altered between 1 and 11. Figure 1

shows the results, based on which, adsorption percentage of Hg (I) and Hg (II) ions ascends as the initial pH of the solution rises, hence at pH=1, the lowest adsorption percentage and at pH=9 and 7, the highest adsorption percentage were obtained for mercury ions (I) and (II), respectively. The reason can be expressed based on the percentages of hydronium ions in the solution. In other words, when pH is low, the concentration of H⁺ ions is high and the competition between H⁺, Hg⁺, and Hg²⁺ ions for adsorption onto the adsorbent surface causes the adsorption, itself, be decreased. But when pH is high, because of reduced H⁺ ions, these ions cannot compete with Hg⁺ and Hg²⁺ ions, hence the adsorption increases.

For the purpose of studying nanoparticles size's effect on adsorption percentage, we utilized titanium dioxide nanoparticles, 20, 100, and 400 nm in size. The highest adsorption percentage was obtained for both mercury ions (I) and (II), with the adsorbent size of 20 nm (Fig. 2). The larger the size of TiO₂ nanoparticles, the smaller the ratio of surface to volume and thus, the fewer the available sites for adsorption and subsequently the lower the adsorption. Available places for adsorption and contact region area of particles with absorbent surface of 20 nm nanoparticles are more than 100 and 400 nm, hence more ions are probable to be absorbed on the surface and will have maximum adsorption percentage.

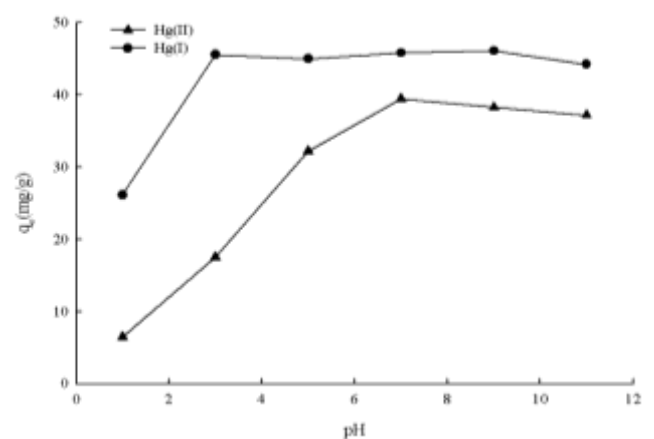


Fig. 1. The effect of initial pH of the solution on the adsorption percentage (constant conditions: initial concentration of the solution 50 mg/L for Hg(I) and 40 mg/L for Hg(II), with particle size of 20 nm, temperature of 22±1°C, contact time of 45 min, and adsorbent dosage of 0.05g)

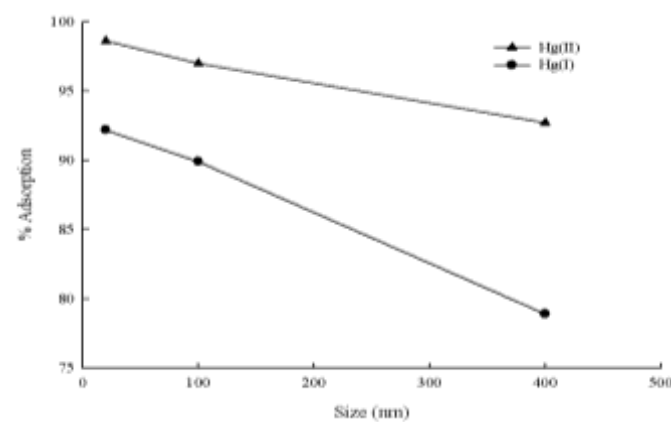


Fig. 2. The effect of particle size on adsorption percentage (constant conditions: initial concentration of the solution = 50 mg/L for Hg(I) and 40 mg/L for Hg(II), pH=9 for Hg(I) and pH=7 for Hg(II), temperature=22±1°C, contact time=45 min, and adsorbent dosage=0.05g)

Figure 3 illustrates the impact of TiO₂ nanoparticles' quantity on the adsorption of mercury (I) and (II) ions. Results show that the amount of 0.05 g of titanium dioxide nanoparticles is optimal value for maximum adsorption of mercury (I) and (II) ions from the aqueous solution. The adsorption percentage ascends as the adsorbent quantity grows, which is due to the increase in effective collisions between mercury ions and TiO₂ nanoparticles.

Figure 4 shows the impact of contact time on adsorption percentage of mercury (I) and (II) ions onto titanium dioxide nanoparticles, examined at 15, 30, 45, 60, 75, 90, and 105 minutes.

As seen, by increasing the contact time, the adsorption percentages of mercury (I) and (II) ions in the solution will ascend respectively, up to 75 minutes and 45 minutes, because mercury ions have more times for adsorption onto the adsorbent.

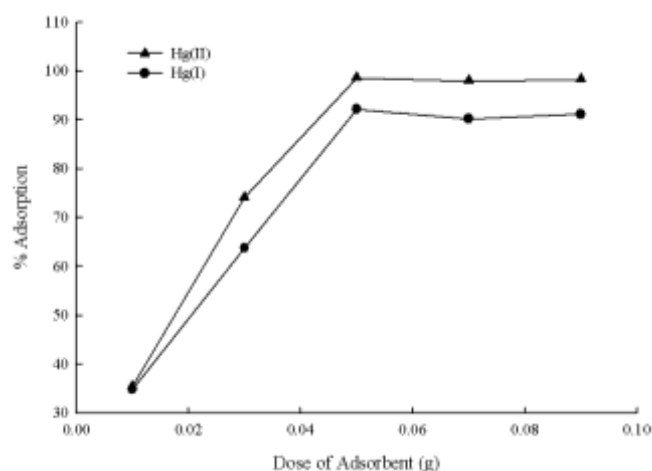


Fig. 3. The effect of adsorbent dosage on the adsorption percentage (constant conditions: initial concentration of the solution 50 mg/L for Hg(I) and 40 mg/L for Hg(II), pH 9 for Hg(I) and pH 7 for Hg(II), particle size 20 nm, contact time 45 min and temperature 22±1 C)

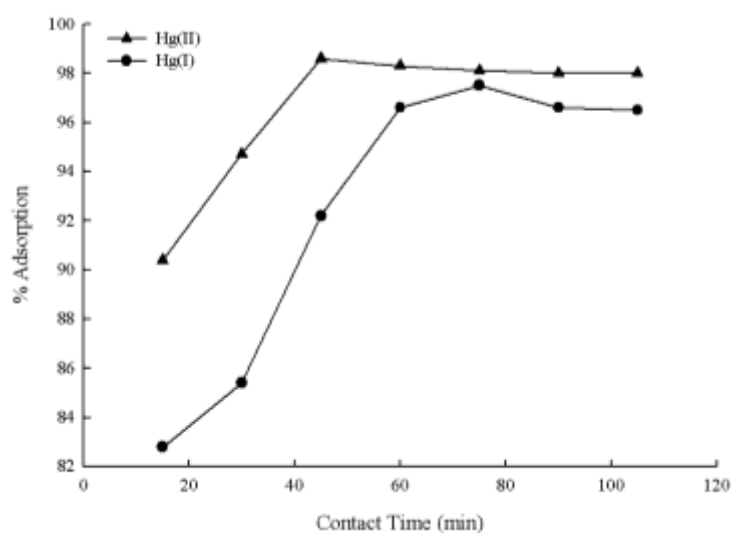


Fig. 4. The effect of contact time on the adsorption percentage (constant conditions: initial concentration of the solution 50 mg/L for Hg(I) and 40 mg/L for Hg(II), pH 9 for Hg(I) and pH 7 for Hg(II), particle size 20 nm, temperature 22±1 C and adsorbent dosage 0.05g)

To evaluate the effect of temperature, the adsorption experiments were performed at different temperatures of 22°C, 35°C, 45°C, and 55°C. Figure 5 demonstrates the results. As it can be seen, the highest adsorption percentage was obtained for both mercury ions at temperature of 22°C. Adsorption percentage is reduced as the temperature increases, because adsorption process of mercury ions (I) and (II) on titanium dioxide nanoparticles is exothermic, similar to the most of adsorption processes.

The initial concentration of adsorbate is a factor that can affect the adsorption. As the data in Figure 6 show, the adsorption percentage is decreased by increasing initial concentration of Hg (I) and Hg (II) ions so that initial concentration of 50 and 40 mg/L is more satisfactory, respectively. The reason for this is that by increasing the adsorbate on adsorbent, the adsorption sites saturate quickly and the adsorption is reduced.

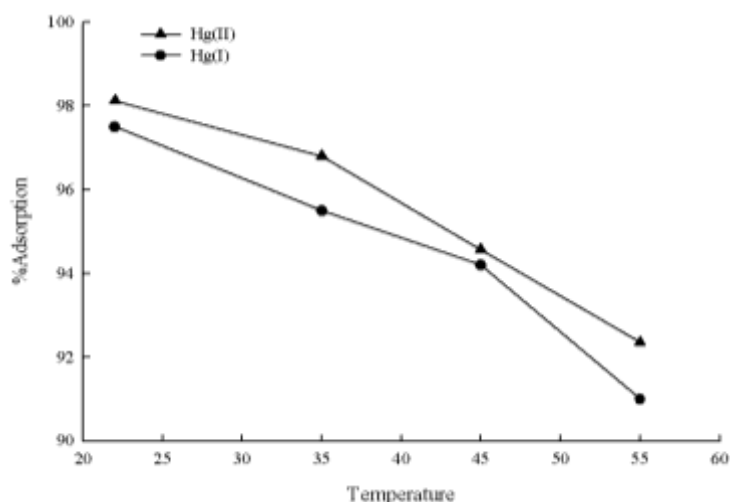


Fig. 5. The effect of temperature on the adsorption percentage (constant conditions: initial concentration of the solution 50 mg/L for Hg(I) and 40 mg/L for Hg(II), pH 9 for Hg(I) and pH 7 for Hg(II), particle size 20 nm, contact time 75 min for Hg(I) and 45 min for Hg(II) and adsorbent dosage 0.05g)

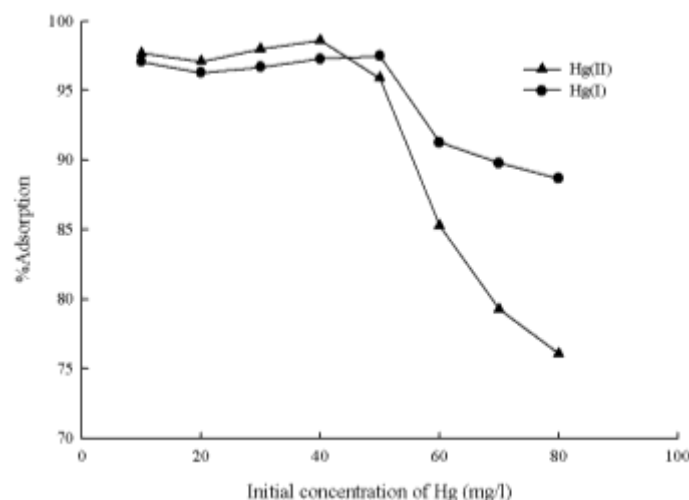


Fig. 6. The effect of initial concentration of Hg (I) and Hg(II) ions on the adsorption percentage (constant conditions: pH=9 for Hg(I) and pH=7 for Hg(II), particle size=20 nm, temperature=22±1 °C, contact time=75 min for Hg(I) and 45 min for Hg(II), and adsorbent dosage=0.05g)

When studying adsorption, in order to have fitting experimental results with theoretical models, adsorption isotherms have been used. Here, the used isotherms were Langmuir, Freundlich, and Temkin isotherms. This linear equations are (He et al., 2015; Mihaly-Cozmuta et al., 2014):

$$\text{Langmuir equation: } \frac{1}{q_e} = \frac{1}{q_m} + \left(\frac{1}{q_m K_L} \right) \frac{1}{C_e} \quad (3)$$

$$\text{Freundlich equation: } \log q_e = \log K_F + \frac{1}{n} \log C_e \quad (4)$$

$$\text{Temkin equation: } q_e = B_1 \ln C_e + B_1 \ln K_T \quad (5)$$

where C_e (mg/L) is the equilibrium concentration of adsorbate in solution; q_e (mg/g), the amount of adsorbate per unit mass of adsorbent; K_L (L/mg), the Langmuir isotherm constant; q_m (mg/g), the maximum adsorption capacity of Langmuir isotherm; K_F ($\text{mg}^{-1-(1/n)} \text{L}^{1/n} / \text{g}$), the Freundlich constant; and n , the intensity of adsorption. Furthermore, $B_1 = \frac{RT}{b}$ is a constant, depending on the adsorption heat and K_T (L/g) is the Temkin isotherm constant.

For Langmuir isotherm, the plot of $1/q_e$ versus $1/C_e$ gives a straight line, in which

K_L is determined by a slope ($\frac{1}{q_m K_L}$) and q_m by an intercept ($1/q_m$) (Fig. 7). For Freundlich isotherm, the plot of $\log q_e$ versus $\log C_e$ gives a straight line in which n is determined by a slope ($1/n$) and K_F by an intercept ($\log K_F$) (Fig. 8). Also, for Temkin isotherm, the plot of q_e versus $\ln C_e$ gives a straight line where B_1 is determined by a slope (B_1) and K_T by an intercept ($B_1 \ln K_T$) (Fig. 9). Table 1 and 2 show the results.

The essential characteristic of Langmuir isotherm is represented by using an equilibrium parameter, separation factor (R_L), which is a dimensionless constant, according to Equation (6) (Sheela et al., 2012):

$$R_L = \frac{1}{1 + K_L C_i} \quad (6)$$

where K_L is the Langmuir constant and C_i , the initial concentration of the adsorbate in the solution. This parameter is used to study Langmuir isotherm ability. Table 3 gives information about this equilibrium parameter.

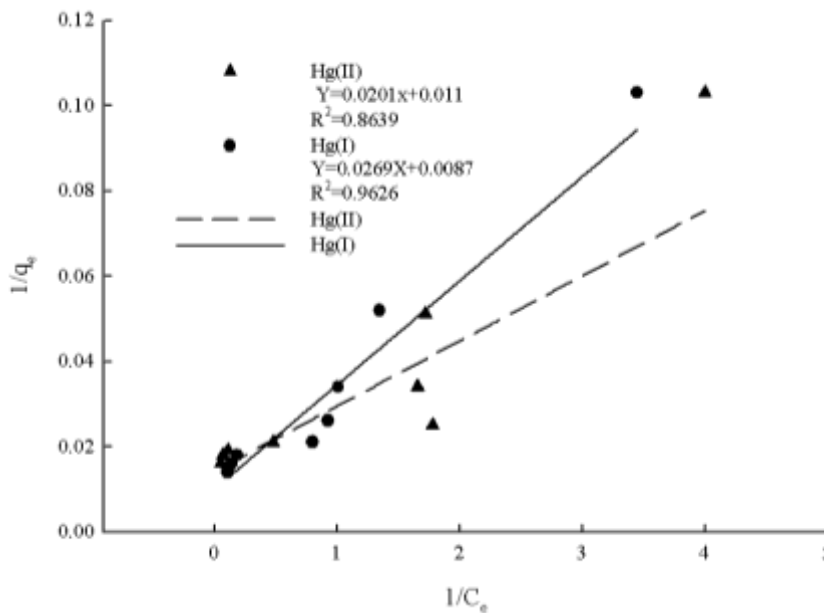


Fig. 7. Langmuir adsorption isotherm for Hg (I) and Hg (II) ions onto TiO₂ nanoparticles

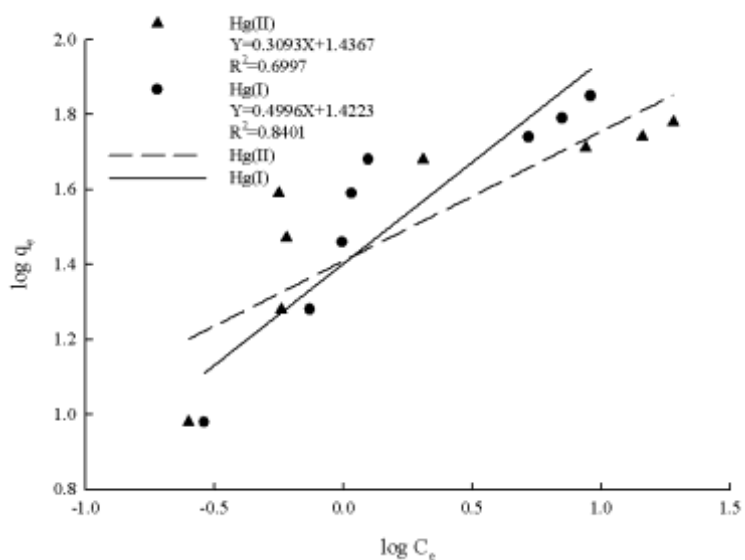


Fig. 8. Freundlich adsorption isotherm for Hg (I) and Hg (II) ions onto TiO₂ nanoparticles

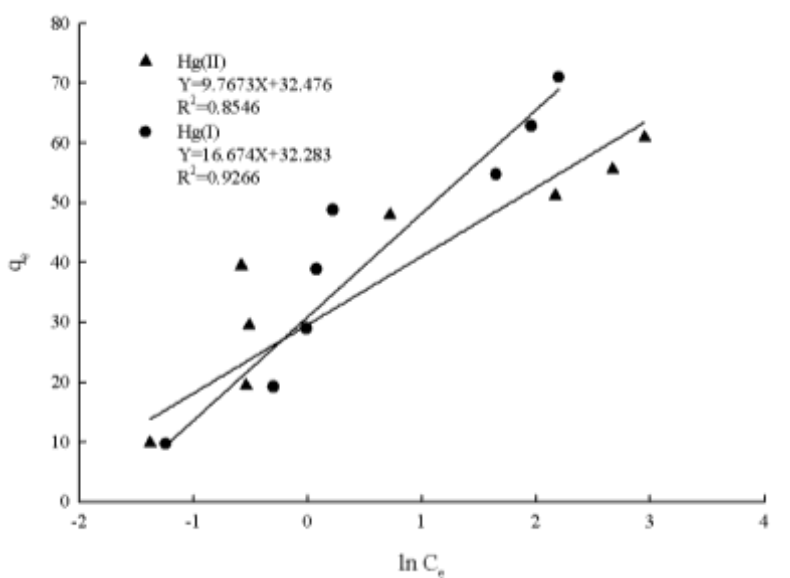


Fig. 9. Temkin adsorption isotherm for Hg (I) and Hg (II) ions onto TiO₂ nanoparticles

Table 1. Parameters of isotherms for Hg(I) ion, using TiO₂ nanoparticles

Langmuir			Freundlich			Temkin		
K _L (L/mg)	q _m (mg/g)	R ²	K _F (mg ^{1-(1/n)} L ^{1/n} /g)	n	R ²	K _T (L/g)	B ₁	R ²
0.32	114.9	0.9626	26.4	2	0.8401	6.9	16.7	0.9266

Table 2. Parameters of isotherms for Hg(II) ion, using TiO₂ nanoparticles

Langmuir			Freundlich			Temkin		
K _L (L/mg)	q _m (mg/g)	R ²	K _F (mg ^{1-(1/n)} L ^{1/n} /g)	n	R ²	K _T (L/g)	B ₁	R ²
0.55	90.9	0.8639	27.3	3.2	0.6997	27.6	9.7	0.8546

Table 3. R_L values and nature of the process

R_L value	Nature of the process
$R_L > 1$	Unfavorable
$R_L = 1$	Linear
$0 < R_L < 1$	Favorable
$R_L \rightarrow 0$	irreversible

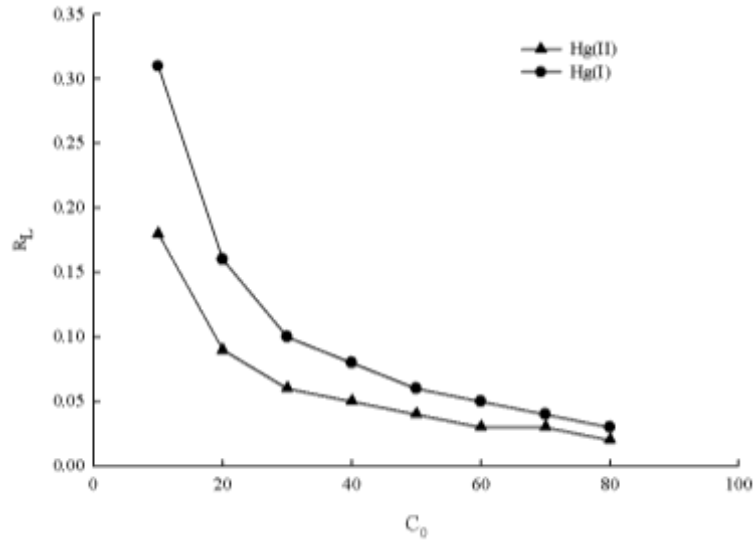


Fig. 10. Separation factor for the adsorption of Hg (I) and Hg (II) ions onto TiO_2 nanoparticles

Figure 10 illustrates the values of this parameter against the initial concentration of mercury ions in the solution. Obtained values of R_L are within the range of 0-1, thus Langmuir-isotherm-based adsorption is favorable.

Studying a reaction usually starts with thermodynamic studies that can predict feasibility or infeasibility of a reaction. By using thermodynamic equilibrium constant, changes in standard Gibbs free energy (ΔG^0) for adsorption at a given temperature can be determined from the following equation (Dashti Khavidaki & Aghaie, 2013; Dashti Khavidaki et al., 2013):

$$\Delta G^0 = -RT \ln K_0 \quad (7)$$

$$K_0 = \frac{q_e}{C_e} \quad (8)$$

where T is the absolute temperature; R (kJ/mol K), the gas constant; and K_0 (L/mol), the thermodynamic equilibrium constant. According to negative values of ΔG^0 in Table 4, it is understood that adsorption process is spontaneous in experiment conditions. When the temperature rises, the tendency for adsorption decreases. Standard enthalpy (ΔH^0) and entropy (ΔS^0) are defined by the following equation (Arshadi et al., 2014):

$$\ln K_0 = \frac{-\Delta H^0}{R} \left(\frac{1}{T} \right) + \frac{\Delta S^0}{R} \quad (9)$$

Table 4. Thermodynamic parameters for the adsorption of Hg(I) and Hg (II) ions onto TiO_2 nanoparticles

T(K)	ΔG^0 (kJ/mol)		ΔH^0 (kJ/mol)		ΔS^0 (J/mol K)	
	Hg(I)	Hg(II)	Hg(I)	Hg(II)	Hg(I)	Hg(II)
295	-8.97	-10.42	-32.15	-43.81	-78.35	-113.16
308	-7.81	-8.73				
318	-7.35	-7.56				
328	-6.29	-6.76				

Standard enthalpy and entropy is obtained from plot of $\ln K_0$ versus $\frac{1}{T}$ (Fig. 11). The slope of this line is $\frac{-\Delta H^0}{R}$ and its intercept, $\frac{\Delta S^0}{R}$, in which ΔH^0 and ΔS^0 can be calculated. As shown in Table 4, according to negative values of standard enthalpy and entropy, it can be concluded that firstly, adsorption processes of both mercury (I) and mercury (II) ions onto TiO_2 nanoparticles is exothermic and secondly, these adsorption processes are associated with reduced disorder.

One of the most important studies concerning the adsorption process are known as kinetics studies, which check the

effect of contact time with the adsorption percentage. Adsorption kinetics model is presented based on the reaction of the pseudo-first order by Lagergren (El-Halwany, 2010).

$$\ln(q_e - q_t) = \ln q_e - K_1 t \quad (10)$$

where K_1 (/h) is the Lagergren rate constant and q_e and q_t are the amounts of mercury ions adsorbed per unit mass of the adsorbent at equilibrium and time t , respectively. In these experiments, plot of $\ln(q_e - q_t)$ versus t , shown in Figure 12, is not a straight line; thus, the adsorption of mercury (I) and (II) ions onto titanium dioxide nanoparticles are not the pseudo-first order.

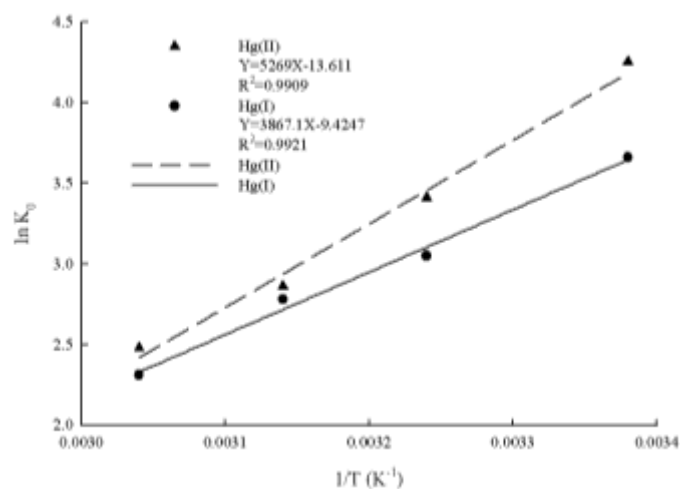


Fig. 11. Plot of $\ln K_0$ versus $\frac{1}{T}$ for the Thermodynamic parameters for the adsorption of Hg(I) and Hg (II) ions onto TiO_2 nanoparticles

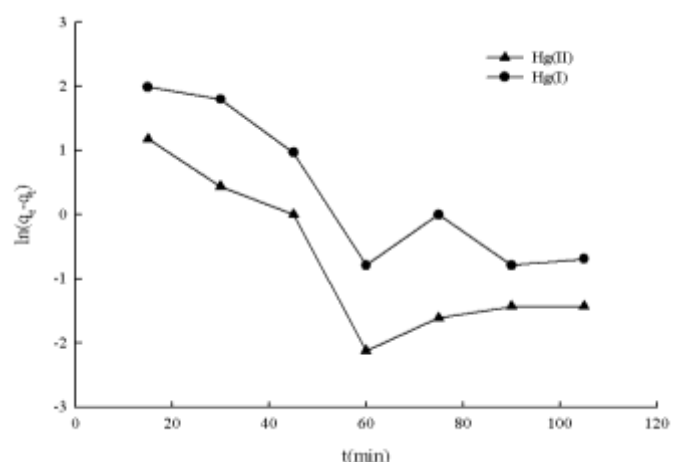


Fig. 12. Pseudo-first order kinetics for the adsorption of Hg(I) and Hg (II) ions onto TiO_2 nanoparticles

The pseudo-second order mechanism by Ho et al. is presented (El-Halwany, 2010):

$$\frac{t}{q_t} = \frac{1}{k_2 q_e^2} + \frac{1}{q_e} t \quad (11)$$

where K_2 is a constant rate for pseudo-second order equation, obtained from plot of t/q_t versus t (min). The slope of this straight line is $\frac{1}{q_e}$ and its intercept, $\frac{1}{k_2 q_e^2}$, in which k_2 and q_e can be calculated (Fig. 13). In accordance to the plot, the adsorption of mercury (I) and (II) ions onto titanium dioxide nanoparticles are pseudo-second order with the results, shown in Table 5.

A few nano-adsorbents have been used to remove mercury ions from aqueous solutions. Efficiency of these adsorbents can be compared by the maximum adsorption capacity (q_m), obtained from the related Langmuir isotherm. This parameter shows the maximum value of the adsorbate (mg) onto unit mass of adsorbent (g). The comparison results in Table 6 show that the highest values of q_m are related to titanium dioxide nanoparticles. Therefore, in our opinion, among these nano-adsorbents, titanium dioxide nanoparticles is a more suitable adsorbent for removing mercury ions from aqueous solutions.

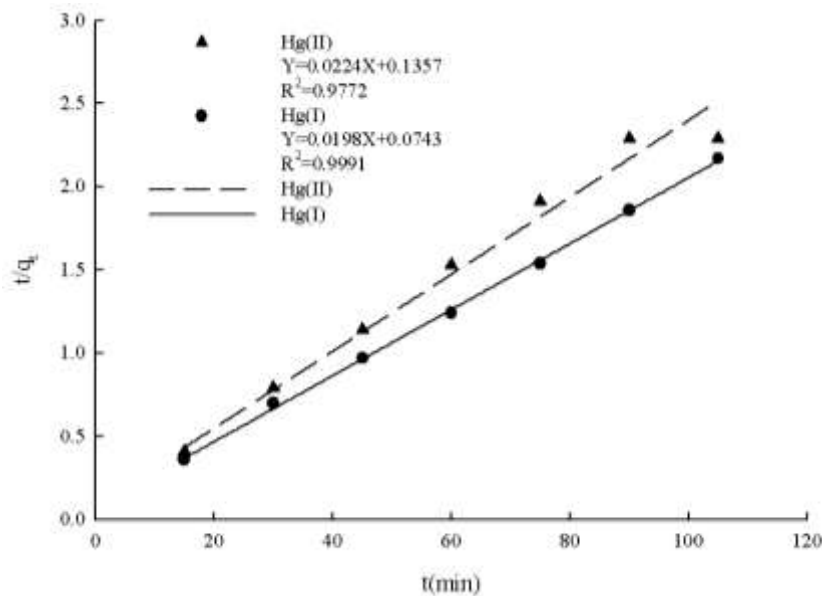


Fig. 13. Pseudo-second order kinetics for the adsorption of Hg(I) and Hg (II) ions onto TiO₂ nanoparticles

Table 5. Parameters of kinetics for Hg(I) and Hg (II) ions onto TiO₂ nanoparticles

K ₂ (mg/g min)		q _e (mg/g)		R ²	
Hg(I)	Hg(II)	Hg(I)	Hg(II)	Hg(I)	Hg(II)
0.0053	0.0037	50.5	44.6	0.999	0.977

Table 6. Comparison of the maximum adsorption capacity for mercury ions adsorption onto a few nano-adsorbents

nano-adsorbents	q _e (mg/g)	Reference
multi-walled carbon nanotubes	25.6	Yaghmaeian et al. (2015)
magnetite-polyrhodanine core-shell nanoparticles	36.6	Rahmanzadeh et al. (2016)
Fe ₃ O ₄ @SiO ₂ -SH nanoparticles	90.0	Wang et al. (2016)
titanium dioxide nanoparticles	90.9	Current Work

CONCLUSION

The results show that TiO₂ nanoparticle is a good adsorbent for removing Hg (I) and Hg (II) ions from aqueous solutions. The optimum conditions for the adsorption of Hg (I) ion onto TiO₂ nanoparticles are as the following: contact time= 75 min; adsorbent dosage= 0.05 g; initial concentration of Hg (I) ion= 50 mg/L; temperature= 22 °C, and pH= 9. In contrast, the optimum conditions for the adsorption of Hg (II) ion onto TiO₂ nanoparticles are: contact time= 45 min; adsorbent dosage= 0.05 g; initial concentration of Hg (II) ions= 40 mg/L; temperature= 22 °C, and pH= 7. Maximum adsorption of Hg (I) and Hg (II) ions onto TiO₂ nanoparticles under the optimum conditions are 97.5% and 98.6%, respectively. Comparison of experimental results with adsorption isotherms of Langmuir, Freundlich and Temkin shows that adsorption of Hg (I) and Hg (II) ions by titanium dioxide nanoparticles corresponds fairly to the Langmuir adsorption isotherm model. The kinetics study of the adsorption process demonstrate that the model of kinetics for adsorption of Hg (I) and Hg (II) ions from aqueous solutions onto TiO₂ nanoparticles corresponds to a pseudo-second order model.

REFERENCES

Arshadi, M., Amiri, M.J. and Mousavi, S. (2014). Kinetic, equilibrium and thermodynamic investigations of Ni(II), Cd(II), Cu(II) and Co(II) adsorption on barley straw ash. *Water Resources and Industry*, 6, 1-17.

Azevedo, B.F., Furieri, L.B., Pecanha, F.M., Wiggers, G.A., Vassallo, P.F., Simoes, M.R., Fiorim, J., Batista, P. R., Fioresi, M., Rossoni, L., Stefanon, I., Alonso, M.J., Salaces, M. and Vassallo, D.V. (2012). Toxic Effects of Mercury on the Cardiovascular and Central Nervous Systems. *Journal of Biomedicine and Biotechnology*, 1-11.

Bae, W., Mehra, R.K., Mulchandani, A. and Chen, W. (2001). Genetic engineering of *Escherichia coli* for enhanced uptake and bioaccumulation of mercury. *Applied and Environment Microbiology*, 67, 5335-5338.

Ballatori, N. and Clarkson, T.W. (1985). Biliary secretion of glutathione and of glutathione-metal complexes. *Fundamental and Applied Toxicology*, 5, 816-831.

Bernhoft, R.A. (2012). Mercury toxicity and treatment: a review of the literature. *Journal of Environmental and Public Health*, 1-10.

Boening, D.W. (2000). Ecological effects, transport, and fate of mercury: a general review. *Chemosphere*, 40, 1335-1351.

Clarkson, T.W. and Magos, L. (2006). The toxicology of mercury and its chemical compounds. *Critical Reviews in Toxicology*, 36, 609-662.

Dabrowski, A. (2001). Adsorption-from theory to practice. *Advances in colloid and interface science*, 93, 135-224.

Dashti Khavidaki, H. and Aghaie, H. (2013). Adsorption of Thallium(I) Ions Using Eucalyptus Leaves Powder. *CLEAN - Soil, Air, Water*, 41, 673-679.

Dashti Khavidaki, H., Aghaie M., Shishehbore, M.R. and Aghaie, H. (2013). Adsorptive removal of thallium (III) ions from aqueous solutions using eucalyptus leaves powder. *Indian Journal of Chemical Technology*, 20, 380-384.

El-Halwany, M. (2010). Study of adsorption isotherms and kinetic models for Methylene Blue adsorption on activated carbon developed from Egyptian rice hull (Part II). *Desalination*, 250, 208-213.

El-Samrani, A., Lartiges, B. and Villiéras, F. (2008). Chemical coagulation of combined sewer overflow: Heavy metal removal and treatment optimization. *Water Research*, 42, 951-960.

Fakhri, A. (2015). Investigation of mercury (II) adsorption from aqueous solution onto copper oxide nanoparticles: Optimization using response surface methodology. *Process Safety and Environmental Protection*, 93, 1-8.

Farooq, U., Kozinski, J.A., Khan, M.A. and Athar, M. (2010). Biosorption of heavy metal ions using wheat based biosorbents-a review of the recent literature. *Bioresource Technology*, 101, 5043-5053.

Fu, F. and Wang, Q. (2011). Removal of heavy metal ions from wastewaters: a review. *Journal of environmental management*, 92, 407-418.

Geier, D.A. and Geier, M.R. (2003). An assessment of the impact of thimerosal on childhood neurodevelopmental disorders. *Pediatric Rehabilitation*, 6, 97-102.

- Grandjean, P., Weihe, P. and White, R.F. (1997). Cognitive deficit in 7-year-old children with prenatal exposure to methylmercury. *Neurotoxicology and Teratology*, 19, 417-428.
- He, C., Ren, L., Zhu, W., Xu, Y. and Qian, X. (2015). Removal of mercury from aqueous solution using mesoporous silica nanoparticles modified with polyamide receptor. *Journal of colloid and interface science*, 458, 229-234.
- Houston, M.C. (2007). The role of mercury and cadmium heavy metals in vascular disease, hypertension, coronary heart disease, and myocardial infarction. *Alternative Therapies in Health and Medicine*, 13, 128-133.
- Hunsom, M., Pruksathorn, K., Damronglerd, S., Vergnes, H. and Duverneuil, P. (2005). Electrochemical treatment of heavy metals (Cu 2+, Cr 6+, Ni 2+) from industrial effluent and modeling of copper reduction. *Water Research*, 39, 610-616.
- Mihaly-Cozmuta, L., Mihaly-Cozmuta, A., Peter, A., Nicula, C., Tutu, H., Silipas, D. and Indrea, E. (2014). Adsorption of heavy metal cations by Na-clinoptilolite: equilibrium and selectivity studies. *Journal of environmental management*, 137, 69-80.
- Namasivayam, C. and Kadirvelu, K. (1999). Uptake of mercury(II) from wastewater by activated carbon from an unwanted agricultural waste by-product: coirpith. *Carbon*, 37, 79-84.
- Nriagu, J.O., Pfeiffer, W.C., Malm, O., Magalhaes De Souza, C.M. and Mierle, G. (1992). Mercury pollution in Brazil. *Nature*, 356, 1-11.
- Ok, Y.S., Yang, J.E., Zhang, Y.S., Kim, S.J. and Chung, D.Y. (2007). Heavy metal adsorption by a formulated zeolite-Portland cement mixture. *Journal of Hazardous Materials*, 147, 91-96.
- Ozaki, H., Sharma, K. and Saktaywin, W. (2002). Performance of an ultra-low-pressure reverse osmosis membrane (ULPROM) for separating heavy metal: effects of interference parameters. *Desalination*, 144, 287-294.
- Pestana, M.H.D. and Formoso, M.L.L. (2003). Mercury contamination in Lavras do Sul, south Brazil: a legacy from past and recent gold mining. *Science of the Total Environment*, 307, 125-140.
- Rahmanzadeh, L., Ghorbani, M. and Jahanshahi, M. (2016). Effective removal of hexavalent mercury from aqueous solution by modified polymeric nanoadsorbent. *Journal of Water and Environmental Nanotechnology*, 1, 1-8.
- Rooney, J.P.K. (2007). The role of thiols, dithiols, nutritional factors and interacting ligands in the toxicology of mercury. *Toxicology*, 234, 145-156.
- Saglam, N., Say, R., Denizli, A., Patır, S. and Arica, M.Y. (1999). Biosorption of inorganic mercury and alkylmercury species on to *Phanerochaete chrysosporium* mycelium. *Process Biochemistry*, 34, 725-730.
- Sheela, T., Nayaka, Y.A., Viswanatha, R., Basavanna, S. and Venkatesha, T.G. (2012). Kinetics and thermodynamics studies on the adsorption of Zn(II), Cd(II) and Hg(II) from aqueous solution using zinc oxide nanoparticles. *Powder Technology*, 217, 163-170.
- Wagner-Dobler, I., Von Canstein, H., Li, Y., Timmis, K.N. and Deckwer, W.D. (2000). Removal of mercury from chemical wastewater by microorganisms in technical scale. *Environmental science & technology*, 34, 4628-4634.
- Wang, Z., Xu, J., Hu, Y., Zhao, H., Zhou, H., Liu, Y., Lou, Z. and Xu, X. (2016). Functional nanomaterials: Study on aqueous Hg(II) adsorption by magnetic Fe₃O₄@SiO₂-SH nanoparticles. *Journal of the Taiwan Institute of Chemical Engineers*, 60, 394-402.
- Yaghmaeian, K., Khosravi Mashizi, R., Nasserli, S., Mahvi, A.H., Alimohammadi, M. and Nazmara, S. (2015). Removal of inorganic mercury from aquatic environments by multi walled carbon nanotubes. *Journal of Environmental Health Science and Engineering*, doi: 10.1186/s40201-015-0209-8.
- Yun, C.H., Prasad, R., Guha, A.K. and Sirkar, K.K. (1993). Hollow fiber solvent extraction removal of toxic heavy metals from aqueous waste streams. *Industrial & engineering chemistry research*, 32, 1186-1195.
- Zalups, R.K. (2000). Molecular interactions with mercury in the kidney. *Pharmacological Reviews*, 52, 113-143.

